Electronic Supplementary Material (ESI) for ChemComm.

Electronic Supporting Information

Efficient oxygen evolving catalyst based on *μ*-O diiron coordination complex

Yongdong Liu[a], Rui Xiang[a], Xiaoqiang Du[a], Yong Ding[a, b] *, Baochun Ma[a] *

[a] State Key Laboratory of Applied Organic Chemistry, College of Chemistry and Chemical Engineering, Lanzhou University, Lanzhou 730000, China.

[b] State Key Laboratory for Oxo Synthesis and Selective Oxidation, Lanzhou Institute of Chemical Physics, Chinese Academy of Sciences, Lanzhou 730000

* To whom correspondence should be addressed.
E-mail addresses: dingyong1@lzu.edu.cn; mabaochun@lzu.edu.cn

Experimental section

Materials:

Meso-Tetra(4-carboxyphenyl)porphine (TCPP), 1,10-phenanthroline (phen), 2,2'-Bipyridine (bpy) were purchased from Frontier Scientific, Inc. Ligands of N,N-Bis(2-pyridylmethyl)-N-(2-hydroxybenzyl)amine (HL1), Tris(2-pyridylmethyl)amine (TPA), complexes of FeTPA (**1**), $[(TPA)_2Fe_2(\mu\text{-}O)Cl_2]Cl_2$ (**2**), $Fe(L1)Cl_2$ (**3**), FeTCPP (**4**), $Fe(bpy)_2Cl_2$ (**5**), $Fe(phen)_2Cl_2$ (**6**) and nano-Fe_2O_3 were synthesized according to published procedures. Purified water (18.25 MΩ.cm) for the preparation of solutions was obtained from a Molecular Lab Water Purifier (Molelement 1018D). 97% O-18 enriched water was purchased from Marshall Isotopes Ltd, Israel. All of other chemicals and salts used were of the highest purity available from commercial sources.

Cyclic Voltammetry

Cyclic voltammetry (CV) was recorded on a CHI600D electrochemical analyzer with a glassy carbon, Ag/AgCl and Pt wire electrode as the working, reference and auxiliary electrodes, respectively, in acetate buffer solutions (pH 4.5, 230 mM). Analyte concentrations were 1 mM. Electrochemical measurements of **1** were carried out at room temperature with a scan rate of 100 mV s^{-1}.

ESI-MS

Mass spectra were performed over an Agilent Technologies MSD SL Trap mass spectrometer using ESI source coupled with an 1100 Series HPLC system.

FT-IR

Infrared spectra (2- 4 wt% sample in KBr pellets) were recorded using a Bruker VERTEX 70v FT-IR spectrometer.

Raman

Raman scattering spectra were taken using a Renishaw Invia Raman microscope. The laser light source was the 514.5 nm line radiation.

Elemental analysis

Elemental analysis of the catalysts was performed on a TJA ICP-atomic emission spectrometer (IRIS Advantage ER/S).

UV-Vis

UV-Vis absorption spectra were recorded on a TU-1810 (Beijing Purkinje General Instrument Ltd.) equipped with a photomultiplier tube detector.

Dynamic light scattering measurements

Dynamic light scattering (DLS) measurements were performed with a Brookhaven Instruments BI-200SM Laser Light Scattering (USA). The DLS instrument used in this study can detect particle sizes ranging from 1 to 6000 nm. The light source for the scattering experiments is a MGL-III-532nm-200mW-13011360 laser. Data were obtained using a scattering angle of 90 ° at room temperature.

Scanning electron microscopy

Scanning electron microscopy (SEM) images of nanoparticles, which were mounted on a copper micro grid coated with elastic carbon, were observed by a JEOLJEM 2100 operating at 200 keV.

Electron paramagnetic resonance spectrometer

EPR spectra were recorded on a Bruker ER200D-SRC10/12 spectrometer equipped with a standard TE_{102} resonator, a NMR gaussmeter (Bruker ERO35M), a frequency counter (Eip Model371). The EPR spectra were recorded with modulation amplitude of 9×10^{-7}T. EPR spectra were recorded at room temperature.

X-Ray crystallography

Single crystals with a quality suitable for X-ray diffraction were mounted at 298 K on AgilentGemini A Ultra with Mo Kα-radiation (λ = 0.71073) for complex **2**; Cu Kα (λ = 1.54184) for complex **3**. Data were measured using ω scans with 10 s frame exposure and 1° frame width. Data collection, indexing and initial cell refinements were all carried out using CrysAlis^{Pro}[1]. The structure was solved and refined using full-matrix least-squares based on F2 with programs SHELXS-97 and SHELXL-97 64 within Olex2.65.

GC-MS

Analyses were performed using an Agilent Series 7890A model chromatograph connected to an Agilent Series 5975C model mass spectrometer operating in electron impact ionization mode. The Agilent Series 5975C model mass spectrometer detector was tuned for maximum sensitivity (quadrupole temperature, 150 ˚C; ion source temperature, 230 ˚C). The single ion mode was used to scan for the ions m/z = 28, 29, 32, 34, 36, 40 with a dwell time of 100ms, resulting in 8.3 cycles per second. The total flow rate into the spectrometer was limited to 0.6 $mL\cdot min^{-1}$. The GC was equipped with a molecular sieve column (30m × 0.32mm × 15μm), and the vaporizing chamber temperature and column temperature were set for 150 ˚C and 60 ˚C, respectively.

Oxygen measurements

Oxygen evolution was carried out under description: A freshly prepared (19 ml) acetate buffer solution of Oxone was transferred to a 28.3 ml, well stirred vessel, which was sealed with a pierceable rubber septum. Then, 1 ml of catalyst solution was held in a round bottom flask. Both containers were deaerated by purging with Ar gas for 5 minutes. The catalyst solution was then transferred into the vessel quickly. The programmed run of analysis of the sample in the headspace was then started until the reaction was finished.

Isotope-labeled experiment

The $H_2{}^{18}O$ of acetate buffer solution (pH 4.5, 0.23 M) containing Oxone and the acetate buffer solution (pH 4.5, 0.23 M) containing complex **2** were deaerated with Helium gas in two quartz flasks that were sealed with a rubber septum. The solution of **2** (final 75 μM) was then transferred into the vessel with Oxone (final 10 mM) quickly. The final composition of the water is 48.5% $H_2{}^{18}O$:51.5% $H_2{}^{16}O$ v:v. After 1 h, 50 μL of gas sample was withdrawn using a gas-tight syringe for gas analysis.

Table S1: Results of the ^{18}O-Isotope-Labeling Experiments Showing relative abundances of nomal air gas and the gas evolved from 42.5% ^{18}O-labeled $H_2{}^{18}O$ of acetate buffer solution (pH 4.5, 0.23 M) containing Oxone (10 mM) and complex **2** (75 μM).

Simple	Peaks			
	$^{28}N_2$	$^{32}O_2$	$^{34}O_2$	$^{36}O_2$
Air[a]	999	305	1	0
Oxone, complex 2[b]	999	574	78	22
Oxone, complex 2[c]		269	77	22
		Relative abundance (%)		
Oxone, complex 2[c]		73	21	6
Theoretical values		33	49	18

[a] the data of the peaks from Figure S1(a). [b] the data of the peaks from Figure S1(b). [c] $^{32}O_2$, $^{34}O_2$ yields corrected for background air using $^{28}N_2$.

Table S2. Iron-based compounds and screening conditions for catalytic oxygen evolution.[a]

Entry	Catalyst	[Catalyst] (μM)	[Oxone] (mM)	O_2 (μmol)	Turnovers per iron[b]
1	FeTPA (**1**)	15	10	36.9	123
2 [c]	FeTPA (**1**)	15	10	24.4	81
3 [d]	FeTPA (**1**)	15	10	15.2	51
4	FeTPA (**1**)	1.5	10	11.6	387
5	FeTPA (**1**)	1.5	95	35.7	1190
6 [e]	FeTPA (**1**)	1.5	10	0.6	—
7	$[(TPA)_2Fe_2(\mu\text{-}O)Cl_2]Cl_2$ (**2**)	7.5	10	37.0	123
8 [f]	$[(TPA)_2Fe_2(\mu\text{-}O)Cl_2]Cl_2$ (**2**)	0.75	95	35.7	1190 (TON=2380)
9	FeL1 (**3**)	15	10	16.6	55
10	FeL1 (**3**)	1.5	10	5.7	190
11	FeTCPP (**4**)	15	10	0.3	—
12	$Fe(bpy)_2Cl_2$ (**5**)	15	10	2.4	8

13 [g]	$Fe(bpy)_2Cl_2$ (**5**)	15	10	2.9	10
14	$Fe(phen)_2Cl_2$ (**6**)	15	10	0.5	—
15	$FeCl_3$	15	10	0.4	—
16	commercial Fe_2O_3	2.5(mg)	10	0.4	—
17	nano-Fe_2O_3	2.5(mg)	10	0.4	—
18	blank	—	10	0.5	—

[a] Reactions were performed in acetate buffer (0.23 M, pH 4.5) with Oxone at 25 ^{o}C. [b]mol O_2 per mol iron. [c] the second run with addition of Oxone. [d] the third run with addition of Oxone. [e] in Britton-Robinson buffer (40 mM, pH 4.5). [f] TON = mol O_2/mol catalyst. [g] catalyst aged for 48 h.

Table S3. Crystal and Refinement Data for Complexes **2** and **3**.[a]

Complex	2	3
Identification code	$[(TPA)_2Fe_2(\mu\text{-}O)Cl_2]Cl_2\cdot 2H_2O$	$Fe(L1)Cl_2$
Empirical formula	$C_{36}H_{40}Cl_4Fe_2N_8O_3$	$C_{19}H_{18}N_3OFeCl_2$
Formula weight	886.26	431.11
Temperature/K	296(2)	293(2)
Crystal system	monoclinic	monoclinic
Space group	C 2/c	$P2_1/n$
a/Å	15.810(6)	10.1072(8)
b/Å	16.507(6)	7.0595(6)
c/Å	16.162(6)	27.895(2)
α/°	90.00	90.00
β/°	110.875(5)	94.764(8)
γ/°	90.00	90.00
Volume/Å^3	3941(2)	1983.5(3)
Z	4	4
ρ_{calc}mg/mm^3	1.494	1.444
m/mm^{-1}	5.369	8.676
F(000)	1824	884.0
Crystal size/mm^3	0.3 × 0.1 × 0.1	0.33 × 0.31 × 0.29
Radiation	Mo Kα (λ = 0.71073)	Cu Kα (λ = 1.54184)
2Θ range for data collection	3.70 to 50.20°	9.086 to 141.168°
Index ranges	$-18 \leq h \leq 18, -19 \leq k \leq 19, -15 \leq l \leq 19$	$-12 \leq h \leq 12, -7 \leq k \leq 8, -23 \leq l \leq 34$
Reflections collected	13820	10011

Independent reflections	3459 [R_{int} = 0.0222, R_{sigma} = 0.0202]	3782 [R_{int} = 0.0539, R_{sigma} = 0.0549]
Data/restraints/parameters	3459/0/248	3782/0/235
Goodness-of-fit on F^2	1.026	1.130
Final R indexes [I>=2σ (I)]	R_1 = 0.0259, wR_2 = 0.0637	R_1 = 0.0693, wR_2 = 0.2119
Final R indexes [all data]	R_1 = 0.0317, wR_2 = 0.0679	R_1 = 0.0782, wR_2 = 0.2243
CCDC number	1019651	1019750

[a] Crystal data for 3 was agree with the reported data appended from ref 11.

Table 4. FT-IR data for Complexes 2−6

Complexes	FT-IR data (cm^{-1})
2	1628 (w), 1604 (s), 1571 (m), 1484 (m), 1313 (w), 1294 (w), 1157 (w), 1100 (m), 1053 (m), 1024 (m), 975 (w), 827(s), 766 (s), 722 (w), 642 (m).
3	1607 (m), 1591 (m), 1572 (w), 1478 (m), 1454 (s), 1441 (m), 1422 (s), 1281 (s), 1097 (w), 1052 (w), 1020 (m), 885 (w), 750 (m), 730 (m).
4	1701 (s), 1637 (s), 1606 (m), 1488 (m), 1404 (w), 1384 (w), 1320 (w), 1261 (w), 1231 (s), 1108 (w), 1016 (w), 985 (w), 781 (m), 716(m).
5	1629 (w), 1598 (s), 1472 (m), 1314 (s), 1157 (w), 1022 (m), 829 (m), 767 (s), 732 (m), 654 (w).
6	1618 (w), 1502 (s)， 1453 (m), 1411 (m), 1325 (w), 1227 (w), 1053 (m), 890 (m), 842 (s), 811 (s), 723 (m).

Table 5. Fe, Cl Elemental analysis for complexes 1-6

Complexes	Fe [%]	Cl [%]
1	12.06	22.59
2	12.68	16.07
3	12.87	16.63
4	6.16	3.89
5	12.54	15.93
6	11.69	14.39

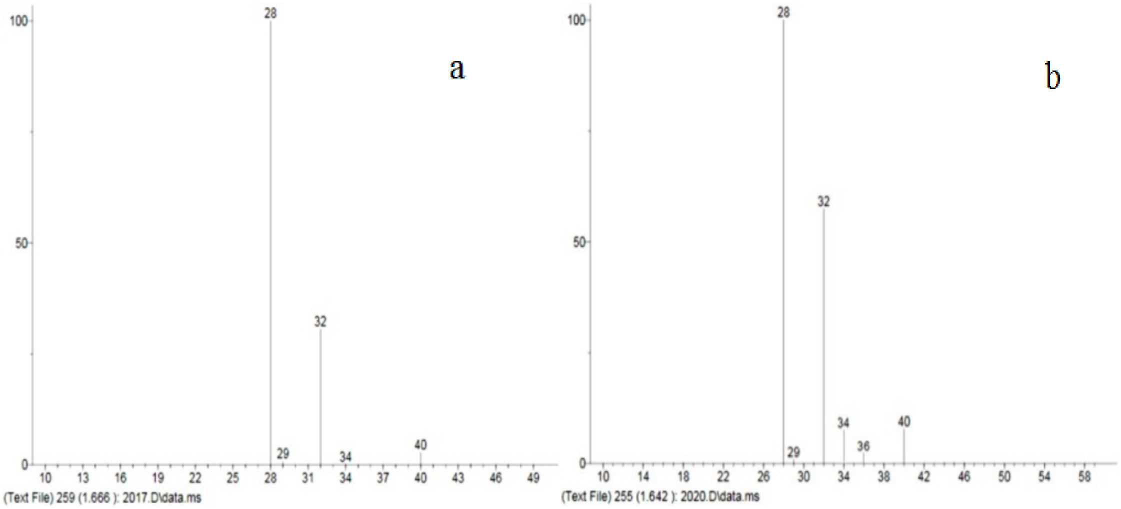

Figure S1. EI mass spectrum of air (a) and the gas sample (b) evolved with the 42.5 atom % $H_2{}^{18}O$ of acetate buffer solution (pH 4.5, 0.23 M) containing Oxone (10 mM) and complex **2** (75 μM). The ions with m/z = 28, 29, 32, 34, 36 and 40 were monitored selectively.

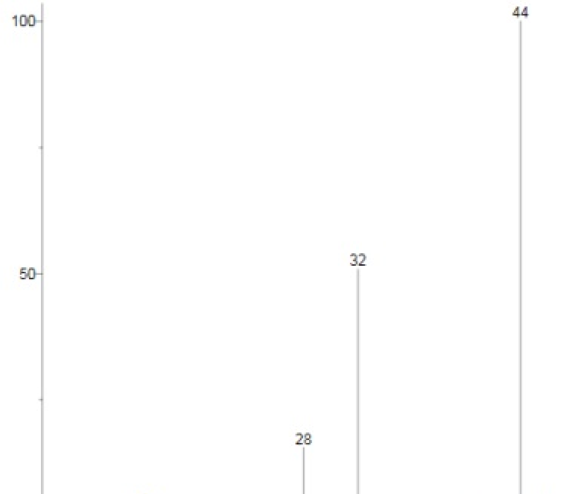

Figure S2. EI mass spectrum of the gas sample evolved with normal H_2O of acetate buffer solution (pH 4.5, 0.23 M) containing Oxone (10 mM) and complex **2** (75 μM). All ions were monitored

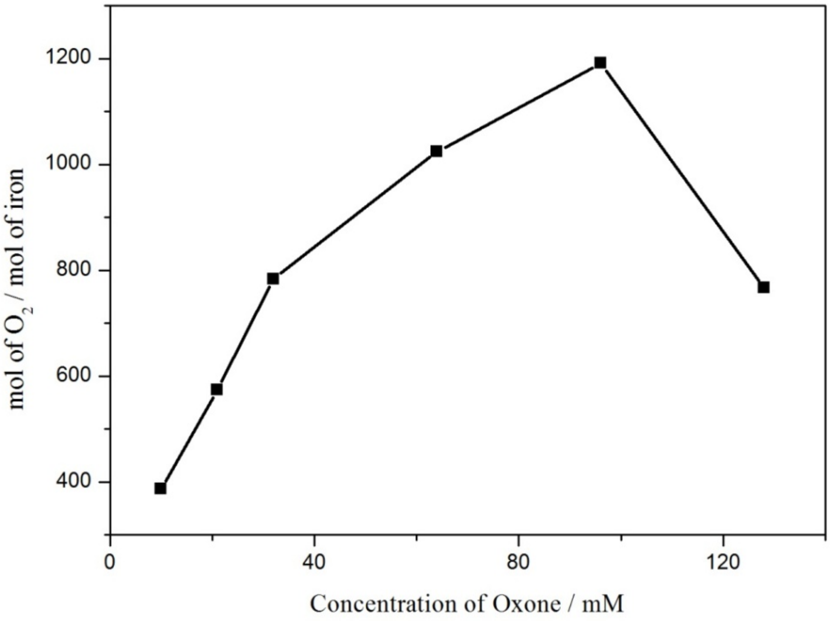

Figure S3**.** Dependence of mol of O_2 per mol of iron on concentrations of Oxone for 80 minutes. Conditions: 1.5 μM FeTPA, 10 – 128 mM Oxone, 0.23 M acetate buffer (initial pH 4.5); total reaction volume 20 mL and overall volume is 28.3 mL; vigorous agitation using a magnetic stirrer.

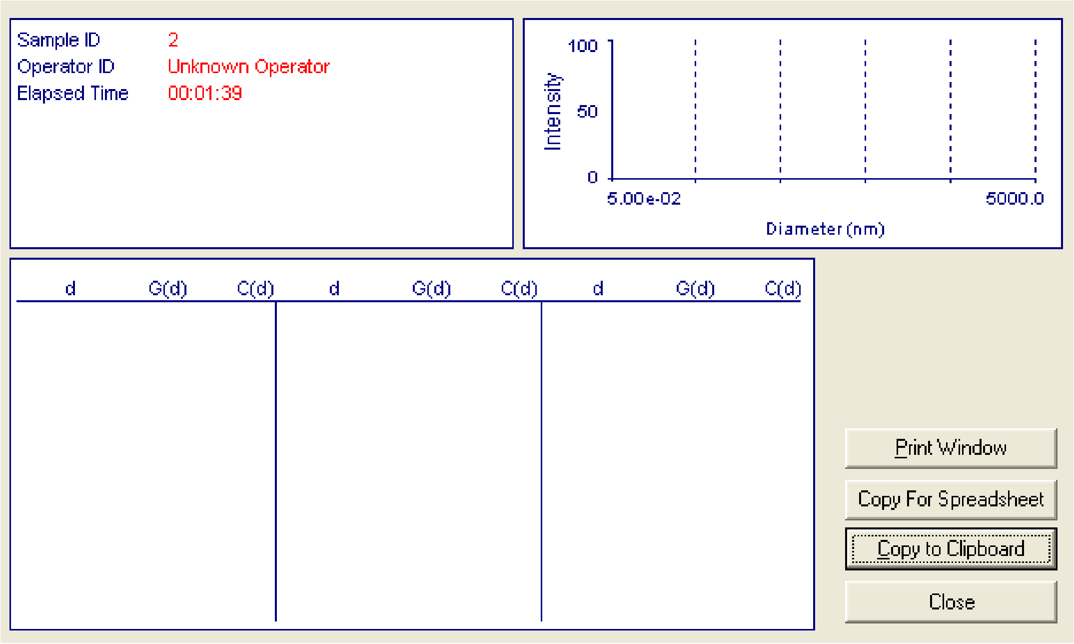

Sample ID 2
Operator ID Unknown Operator
Elapsed Time 00:01:39

d	G(d)	C(d)	d	G(d)	C(d)	d	G(d)	C(d)

Figure S4. Particle size distribution by DLS measurement. **1** (15 μM) in an acetate buffer (0.23 M , pH 4.5) containing Oxone (10 mM) after 80 min of the start of the reaction.

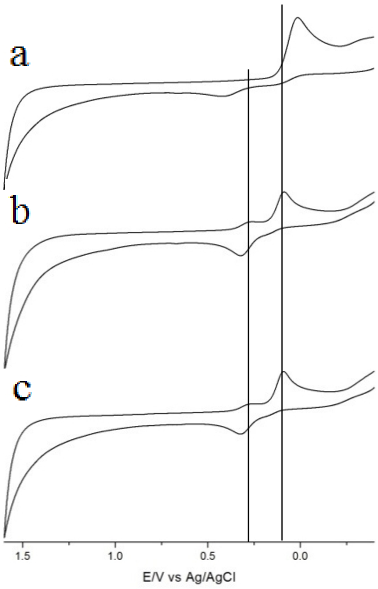

Figure S5. Cyclic voltammogram (CV) of 230 mM acetate buffer solution at pH 4.5 with 1 mM of $Fe(NO_3)_3$ (a), 1 mM of **1** (b) and 0.5 mM of **2** (c). Scan rate: 100 mV s^{-1}.

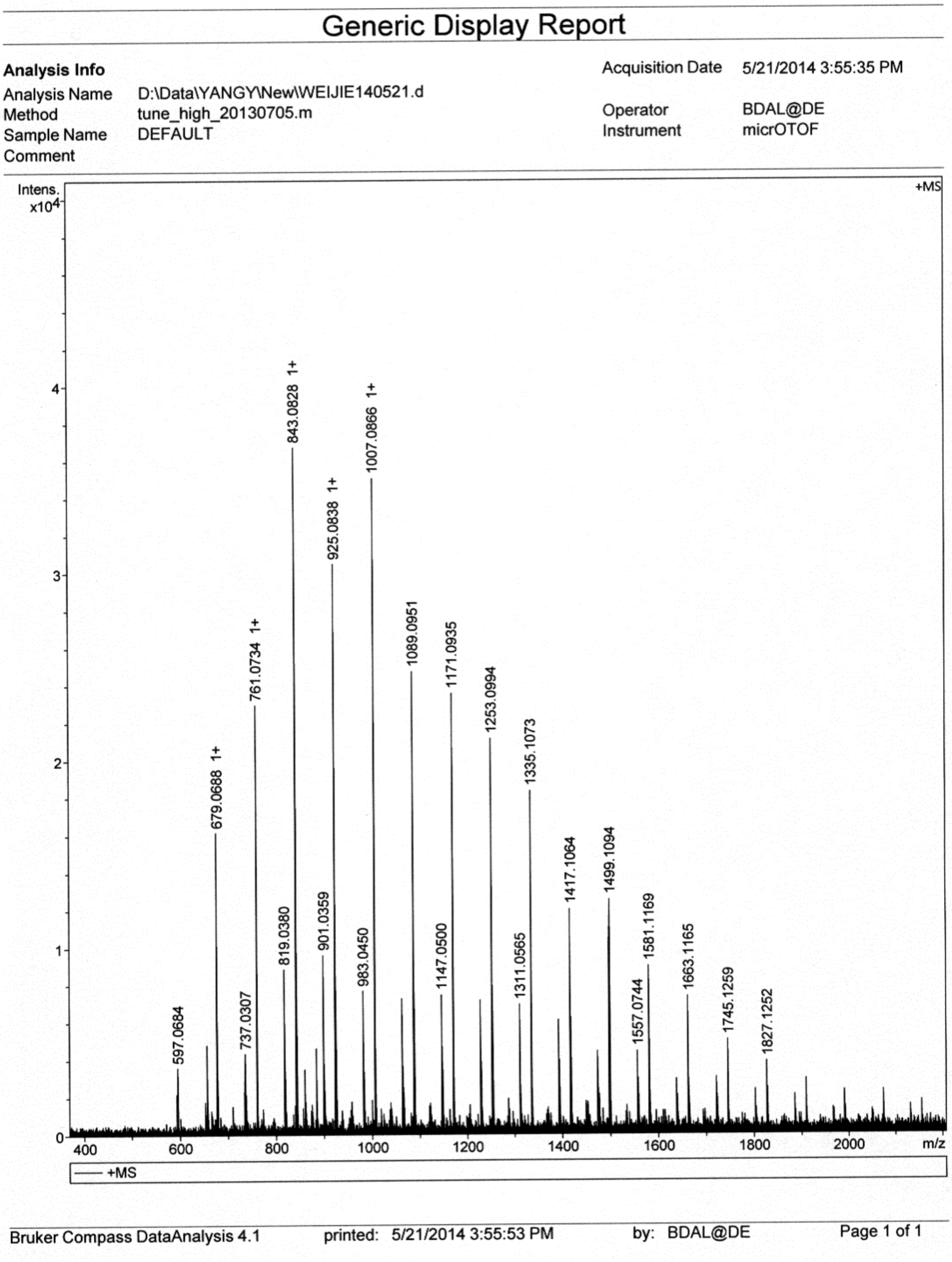

Generic Display Report

Analysis Info		Acquisition Date	5/21/2014 3:55:35 PM
Analysis Name	D:\Data\YANGY\New\WEIJIE140521.d		
Method	tune_high_20130705.m	Operator	BDAL@DE
Sample Name	DEFAULT	Instrument	micrOTOF
Comment			

Bruker Compass DataAnalysis 4.1 printed: 5/21/2014 3:55:53 PM by: BDAL@DE Page 1 of 1

Figure S6. ESI-MS spectrum of complex **2** in acetate buffer solution. The acetate buffer solution (0.23 M, pH 4.5) of **1** and **2** were characterized by ESI-MS. The two complexes ESI-MS performance is the same. However, the ESI mass spectrum shows neither the prominent feature of **1** at m/z 416 nor the feature of **2** at m/z 813. The major new peaks correspond to the $[Fe_2(TPA)_2(\mu\text{-}O)(\mu\text{-}OAc)]$ unit. The major peaks were assigned as follows:

Found 597.0684, $[[Fe_2(TPA)_2(\mu\text{-}O)(\mu\text{-}OAc)]OAc\cdot HOAc\cdot 8H_2O\cdot 2NaOAc]^{2+}$; $(C46H68Fe2N8Na2O19)^{2+}$, m/z 597.16;

Found 679.0688, $[[\mathrm{Fe_2(TPA)_2}(\mu\text{-}\mathrm{O})(\mu\text{-}\mathrm{OAc})]\mathrm{OAc}\cdot\mathrm{HOAc}\cdot 8\mathrm{H_2O}\cdot 4\mathrm{NaOAc}]^{2+}$; $(\mathrm{C50H74Fe2N8Na4O23})^{2+}$, m/z 679.16;

Found 761.0734, $[[\mathrm{Fe_2(TPA)_2}(\mu\text{-}\mathrm{O})(\mu\text{-}\mathrm{OAc})]\mathrm{OAc}\cdot\mathrm{HOAc}\cdot 8\mathrm{H_2O}\cdot 6\mathrm{NaOAc}]^{2+}$; $(\mathrm{C54H80Fe2N8Na6O27})^{2+}$, m/z 761.16;

Found 843.0828, $[[\mathrm{Fe_2(TPA)_2}(\mu\text{-}\mathrm{O})(\mu\text{-}\mathrm{OAc})]\mathrm{OAc}\cdot\mathrm{HOAc}\cdot 8\mathrm{H_2O}\cdot 8\mathrm{NaOAc}]^{2+}$; $(\mathrm{C58H86Fe2N8Na8O31})^{2+}$, m/z 843.16;

Found 925.0838, $[[\mathrm{Fe_2(TPA)_2}(\mu\text{-}\mathrm{O})(\mu\text{-}\mathrm{OAc})]\mathrm{OAc}\cdot\mathrm{HOAc}\cdot 8\mathrm{H_2O}\cdot 10\mathrm{NaOAc}]^{2+}$; $(\mathrm{C62H92Fe2N8Na10O35})^{2+}$, m/z 925.16;

Found 1007.0866, $[[\mathrm{Fe_2(TPA)_2}(\mu\text{-}\mathrm{O})(\mu\text{-}\mathrm{OAc})]\mathrm{OAc}\cdot\mathrm{HOAc}\cdot 8\mathrm{H_2O}\cdot 12\mathrm{NaOAc}]^{2+}$; $(\mathrm{C66H98Fe2N8Na12O39})^{2+}$, m/z 1007.17

Found 1089.0951, $[[\mathrm{Fe_2(TPA)_2}(\mu\text{-}\mathrm{O})(\mu\text{-}\mathrm{OAc})](\mathrm{OAc})_2\cdot\mathrm{HOAc}\cdot 8\mathrm{H_2O}]^{+}$; $(\mathrm{C44H65Fe2N8O17})^{+}$, m/z 1089.32

Found 1171.0935, $[[\mathrm{Fe_2(TPA)_2}(\mu\text{-}\mathrm{O})(\mu\text{-}\mathrm{OAc})](\mathrm{OAc})_2\cdot\mathrm{HOAc}\cdot 8\mathrm{H_2O}\cdot\mathrm{NaOAc}]^{+}$; $(\mathrm{C46H68Fe2N8NaO19})^{+}$, m/z 1171.32

Found 1253.0994, $[[\mathrm{Fe_2(TPA)_2}(\mu\text{-}\mathrm{O})(\mu\text{-}\mathrm{OAc})](\mathrm{OAc})_2\cdot\mathrm{HOAc}\cdot 8\mathrm{H_2O}\cdot 2\mathrm{NaOAc}]^{+}$; $(\mathrm{C48H71Fe2N8Na2O21})^{+}$, m/z 1253.32;

Found 1335.1073, $[[\mathrm{Fe_2(TPA)_2}(\mu\text{-}\mathrm{O})(\mu\text{-}\mathrm{OAc})](\mathrm{OAc})_2\cdot\mathrm{HOAc}\cdot 8\mathrm{H_2O}\cdot 3\mathrm{NaOAc}]^{+}$; $(\mathrm{C50H74Fe2N8Na3O23})^{+}$, m/z 1335.33;

Found 1417.1064, $[[\mathrm{Fe_2(TPA)_2}(\mu\text{-}\mathrm{O})(\mu\text{-}\mathrm{OAc})](\mathrm{OAc})_2\cdot\mathrm{HOAc}\cdot 8\mathrm{H_2O}\cdot 4\mathrm{NaOAc}]^{+}$; $(\mathrm{C52H77Fe2N8Na4O25})^{+}$, m/z 1417.33;

Found 1499.1099, $[[\mathrm{Fe_2(TPA)_2}(\mu\text{-}\mathrm{O})(\mu\text{-}\mathrm{OAc})](\mathrm{OAc})_2\cdot\mathrm{HOAc}\cdot 8\mathrm{H_2O}\cdot 5\mathrm{NaOAc}]^{+}$; $(\mathrm{C54H80Fe2N8Na5O27})^{+}$, m/z 1499.33;

Found 1581.1169, $[[\mathrm{Fe_2(TPA)_2}(\mu\text{-}\mathrm{O})(\mu\text{-}\mathrm{OAc})](\mathrm{OAc})_2\cdot\mathrm{HOAc}\cdot 8\mathrm{H_2O}\cdot 6\mathrm{NaOAc}]^{+}$; $(\mathrm{C56H83Fe2N8Na6O29})^{+}$, m/z 1581.34;

Found 1663.1165, $[[\mathrm{Fe_2(TPA)_2}(\mu\text{-}\mathrm{O})(\mu\text{-}\mathrm{OAc})](\mathrm{OAc})_2\cdot\mathrm{HOAc}\cdot 8\mathrm{H_2O}\cdot 7\mathrm{NaOAc}]^{+}$; $(\mathrm{C58H86Fe2N8Na7O31})^{+}$, m/z 1663.34

Found 1745.1259, $[[\mathrm{Fe_2(TPA)_2}(\mu\text{-}\mathrm{O})(\mu\text{-}\mathrm{OAc})](\mathrm{OAc})_2\cdot\mathrm{HOAc}\cdot 8\mathrm{H_2O}\cdot 8\mathrm{NaOAc}]^{+}$; $(\mathrm{C60H89Fe2N8Na8O33})^{+}$, m/z 1745.34

Found 1827.1252, $[[\mathrm{Fe_2(TPA)_2}(\mu\text{-}\mathrm{O})(\mu\text{-}\mathrm{OAc})](\mathrm{OAc})_2\cdot\mathrm{HOAc}\cdot 8\mathrm{H_2O}\cdot 9\mathrm{NaOAc}]^{+}$; $(\mathrm{C62H92Fe2N8Na9O35})^{+}$, m/z 1827.34

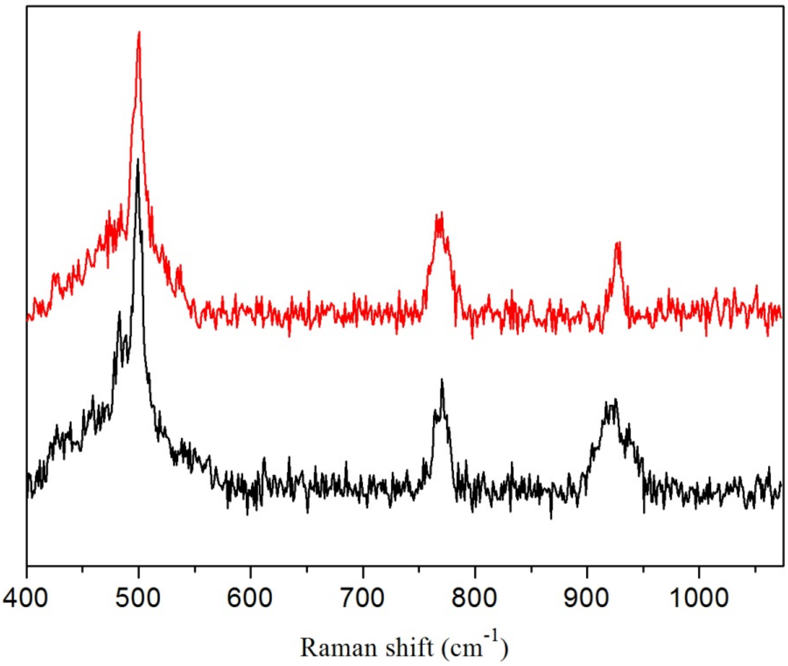

Figure S7. Raman spectra of **1** (red) and **2** (black) solid samples which have treated in acetate buffer solution.

The solid sample of **1** and **2** which have been treated in acetate buffer solution are characterized by Raman spectra. A typical preparation of **1** is as follows: FeTPA **1** was transferred in a round-bottomed flask with acetate buffer solution (0.23M, pH 4.5). The reaction mixture was stirred for a couple of minutes; afterwards the solvent was removed in vacuo. The residue was taken up in a small amount of methanol. The methanol solution was filtered. The solid sample used for Raman characterization was obtained by removing the solvent of the filtrate, and dried in vacuum at room temperature. The dominant characteristic bands at 470-520 cm^{-1} are the typical of oxo-bridged species Fe-O-Fe symmetric stretching mode. The asymmetric stretching mode Fe-O-Fe occurs in the range 750-780 cm^{-1}. The broad band 900-950 cm^{-1} corresponds to the C-C symmetric stretching for residual NaOAc. The frequency of the stretching mode in the monobridged, dibridged and tribridged complexes are consistent with the Fe-O-Fe angle for these complexes.[9, 10] The typical intensity ratio $I_{\mathrm{asym}}/I_{\mathrm{sym}}$ for the (μ-O)(μ-OAc) diiron falls in the range 0.19-0.26 and for (μ-O)bis(μ-OAc) diiron is < 0.1:1. In the resonance Raman spectra, compared with those of the diiron core found in a variety of complexes, the Fe-O-Fe features associated with the dibridged core (μ-O)(μ-OAc)diiron.

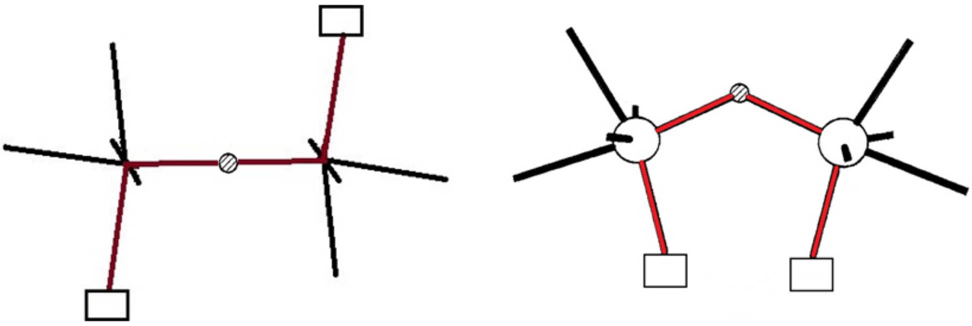

Figure S8. Comparison of complex **2** (left) with trans coordination sites and the dibridged complex [$Fe_2(TPA)_2(O)(OAc)]^{3+}$ (right) with two cis coordination sites.

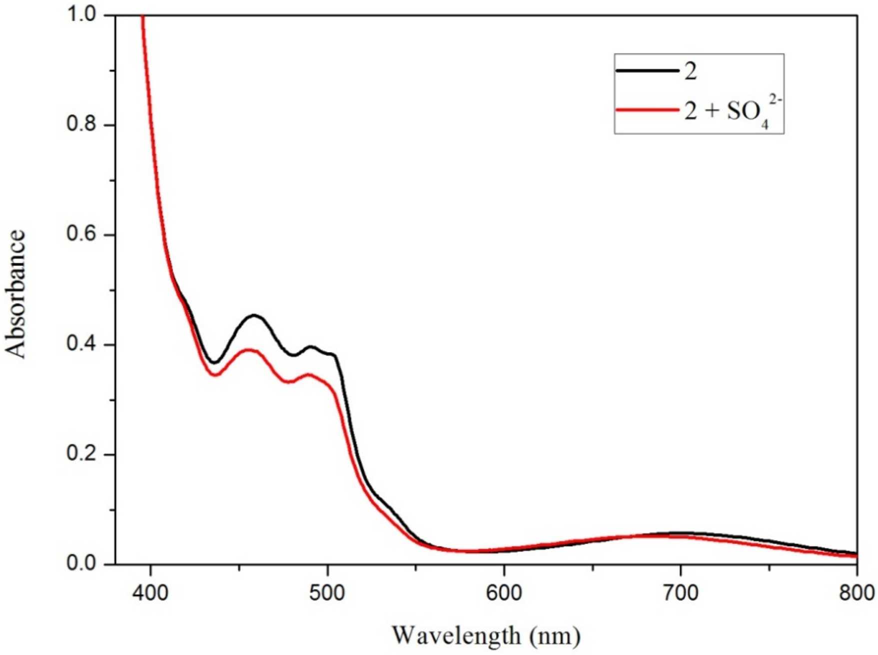

Figure S9. UV-vis spectra before (black) and after (red) addition of 40 equiv of Na_2SO_4 for evolution of **2** (0.5 mM) in acetate buffer.

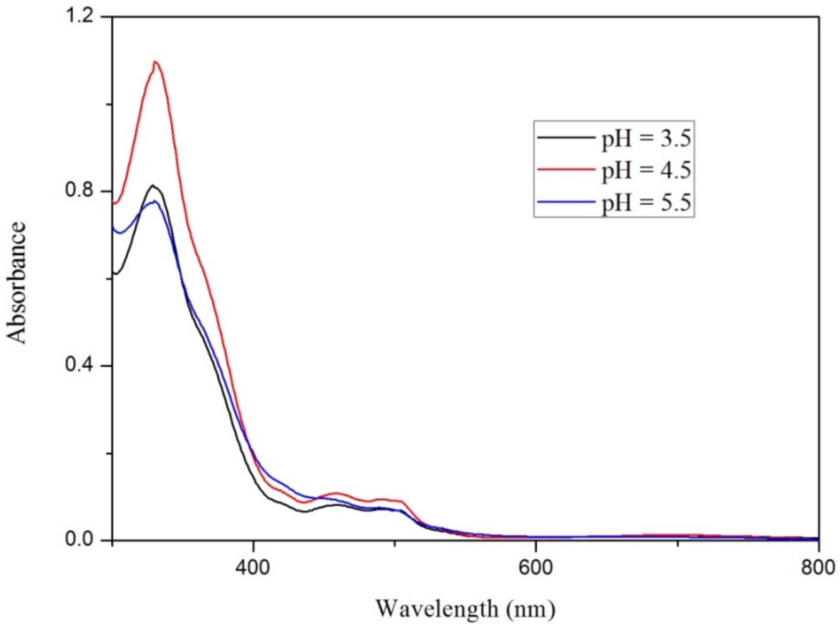

Figure S10. Spectrophotometric titration data of FeTPA (0.4 mM) in 0.23 M acetate buffer with 4 M NaOH. The absorbance spectrum and pH were recorded after each addition.

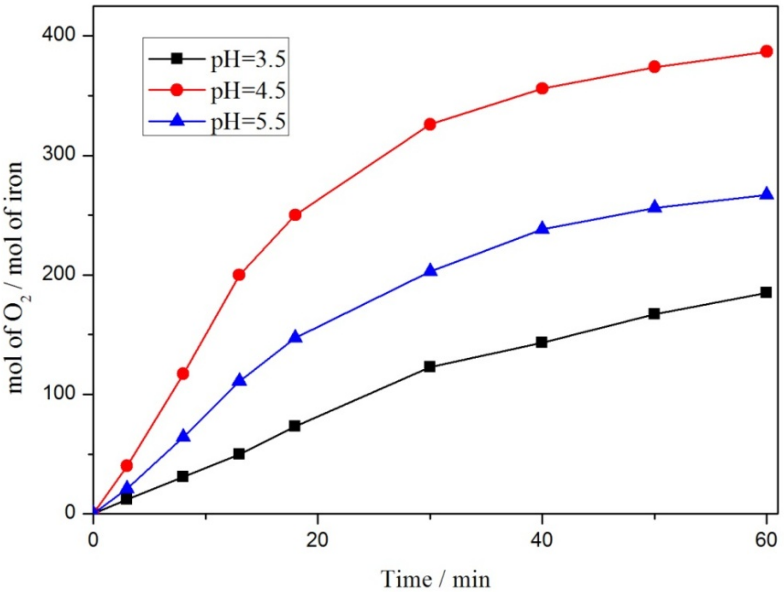

Figure S11. Kinetics of O_2 formation in the presence of 10 mM of Oxone using 1.5 μM of **1** under three pH conditions (0.23 M acetate buffer, initial pH = 3.5, black; pH = 4.5, red; pH = 5.5, blue). Results were obtained after subtraction of the corresponding blank.

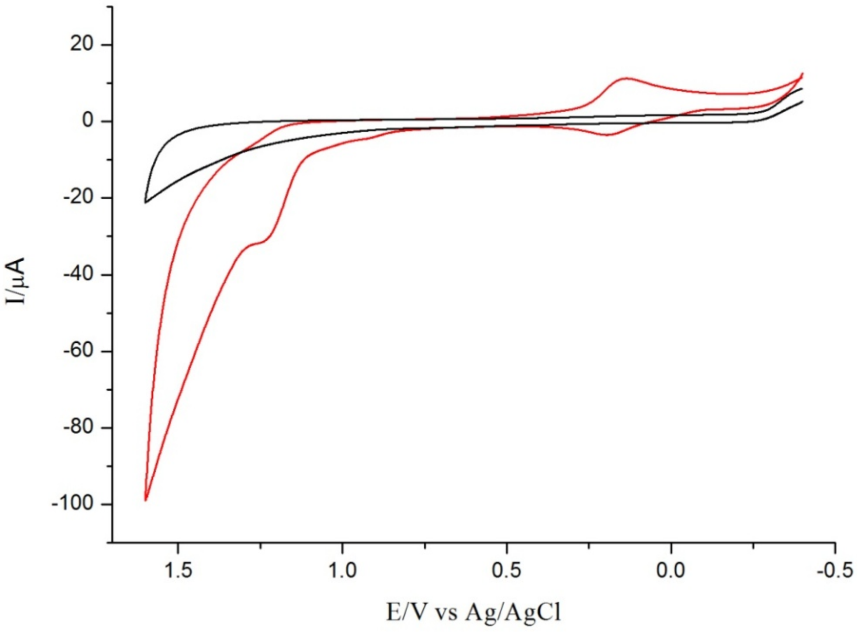

Figure S12. Cyclic voltammogram (CV) of 230 mM acetate buffer solution at pH 4.5 with 1 mM of **3**. Scan rate: 100 mV s^{-1}. Black curve is blank run and red curve is for compound **3**.

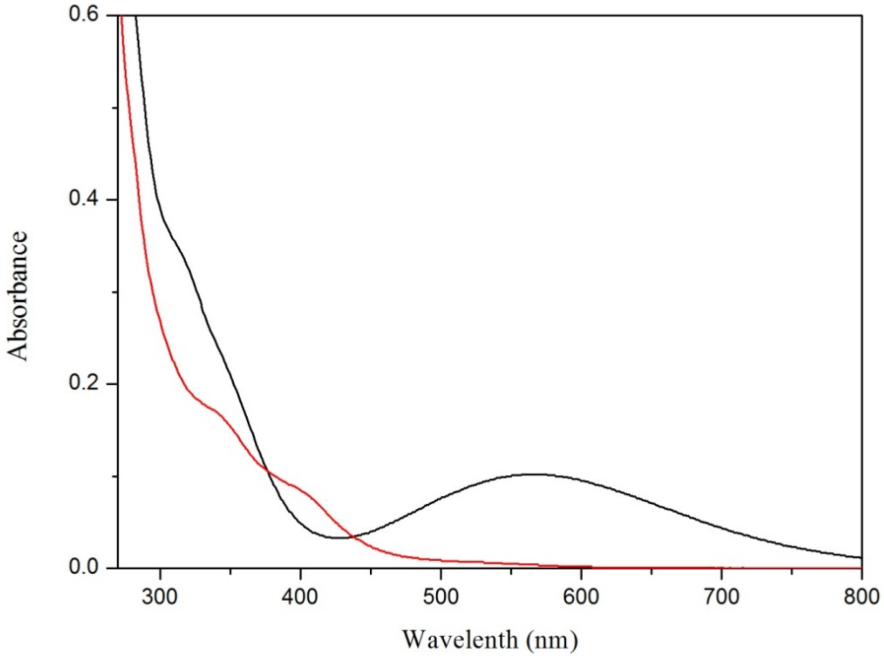

Figure S13. UV-vis spectra before (black) and after (color) addition of 20 equiv of Oxone for evolution of **3** (0.06 mM) in acetate buffer.

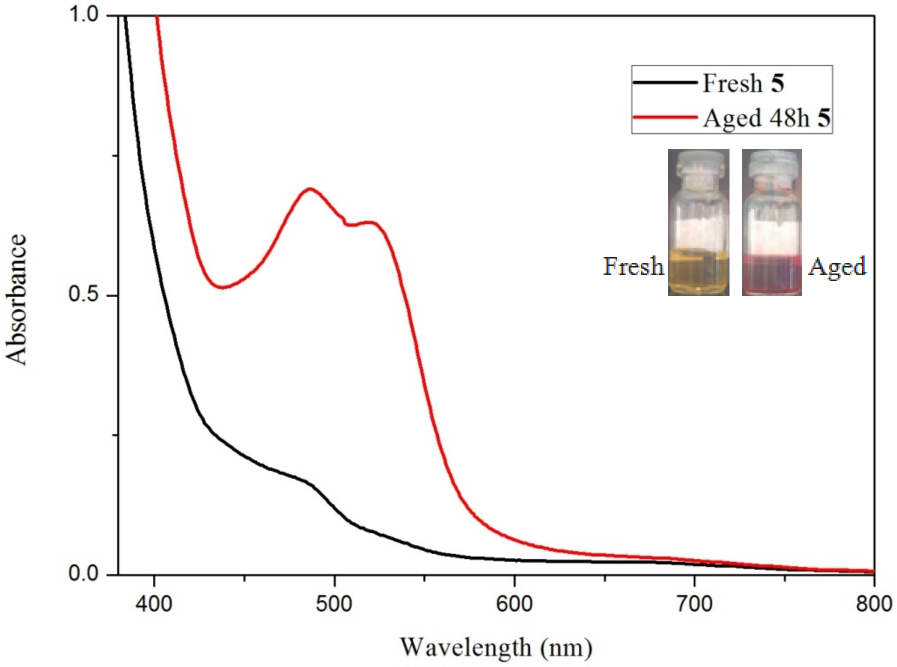

Figure S14. UV-vis spectra for 1.0 mM fresh (black) and 48 h aged 5 (red).

Synthesis of N,N-Bis(2-pyridylmethyl)amine:[1]

To a solution of 2-aminomethylpyridine (2.7 g, 25.0 mmol) in MeOH (50 ml) was added 2-pyridinecarboxaldehyde (2.67 g, 25.0 mmol). A dark brown mixture developed immediately. After stirring at room temperature for 10 h, sodium borohydride (1.89 g, 50 mmol) was added slowly. The brown mixture turned to a pale yellow solution during the addition and stirring was continued for another 2 h. All the volatiles were then removed under reduced pressure. Water (50 ml) was added and the resulting aqueous solution was neutralised with 32% hydrochloric acid, followed by extraction with CH_2Cl_2 (3 × 100 ml). The combined organic extract was dried over anhydrous $MgSO_4$ and rotary evaporated to give a yellow liquid which was used directly for the following reactions without purification. Yield: 4.9 g (99%). ^{1}H NMR (400MHz, $CDCl_3$): δ8.52 (d, J = 4.4 Hz, 2H), 7.60 (t, J =7.6 Hz, 2H), 7.25 (d, J = 7.6 Hz, 2H), 7.12 (t, J =6.0 Hz, 2H), 3.96 (s, 4H,), 3.06 (s, 1H). ^{13}C NMR (400 MHz, $CDCl_3$):159.66, 149.34, 136.57, 122.38, 122.04, 54.78; ESI-MS, (C12H14N3)+, m/z 200.12; found: 200.0667.

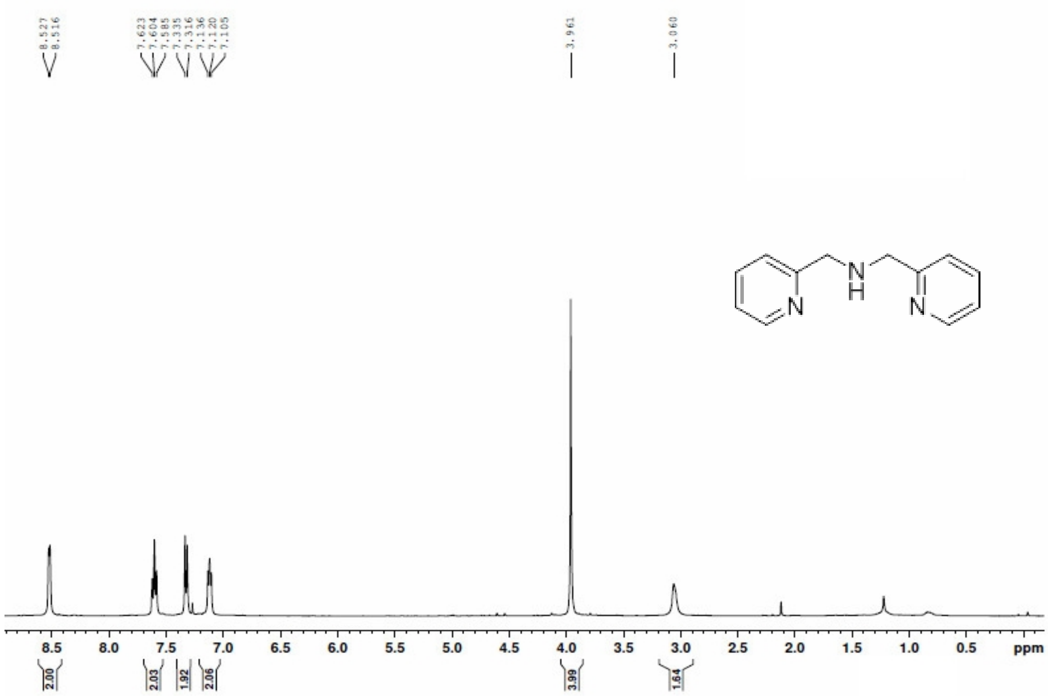

Figure S15. ^{1}H NMR spectrum of N,N-Bis(2-pyridylmethyl)amine

Figure S16. ^{13}C NMR spectrum of N,N-Bis(2-pyridylmethyl) amine.

Synthesis of Tris(2-pyridylmethyl)amine TPA:[2]

5.0 g (25.0 mmol) of N,N-bis(2-pyridylmethyl)amine, 3.0 g (28 mmol) of 2-pyridinecarboxaldehyde and 4.1 ml (4.3 g, 71.67 mmol) of acetic acid were dissolved in 100 ml of methanol. At 0 °C a suspension of 1.5 g (25 mmol) of sodium cyanoborohydride in 75 ml of methanol was added and the reaction mixture was stirred for 72 h. For the workup hydrochloric acid was added to destroy unreacted sodium cyanoborohydride and afterwards the solvent was removed in vacuo. The residue was taken up in water and the pH was adjusted to 9. An oil precipitated which was extracted with dichloromethane (4 x 50 ml). The combined organic layers were dried over $MgSO_4$ and the solvent was removed. The product was obtained as a yellow flaky crystal after recrystallisation from diethyl ether. Yield: 4.3 g (14.8 mmol; 59 %) ^{1}H-NMR (400 MHz, $CDCl_3$): δ (ppm): 8.53 (d, J = 4.0 Hz, 3H), 7.65 (td, J = 8.0, 2.0 Hz, 3H), 7.58 (d, J = 7.6 Hz, 3H), 7.14 (td, J = 6.0, 0.8 Hz, 3H), 3.87 (s, 6H). ^{13}C NMR (400 MHz, $CDCl_3$): 159.43, 149.24, 136.67, 123.13, 122.22, 60.30; ESI-MS, $(C18H19N4)^+$, m/z 291.16; found:291.0865.

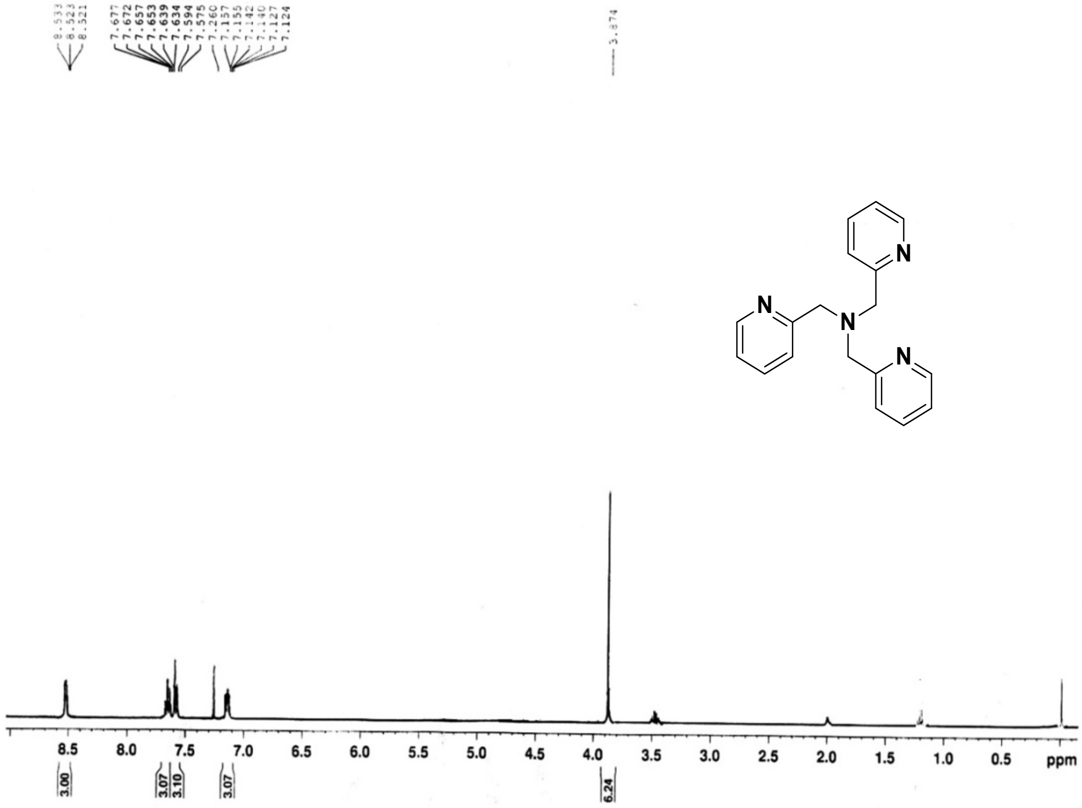

Figure S17. ^{1}H NMR spectrum of Tris(2-pyridylmethyl)amine (TPA).

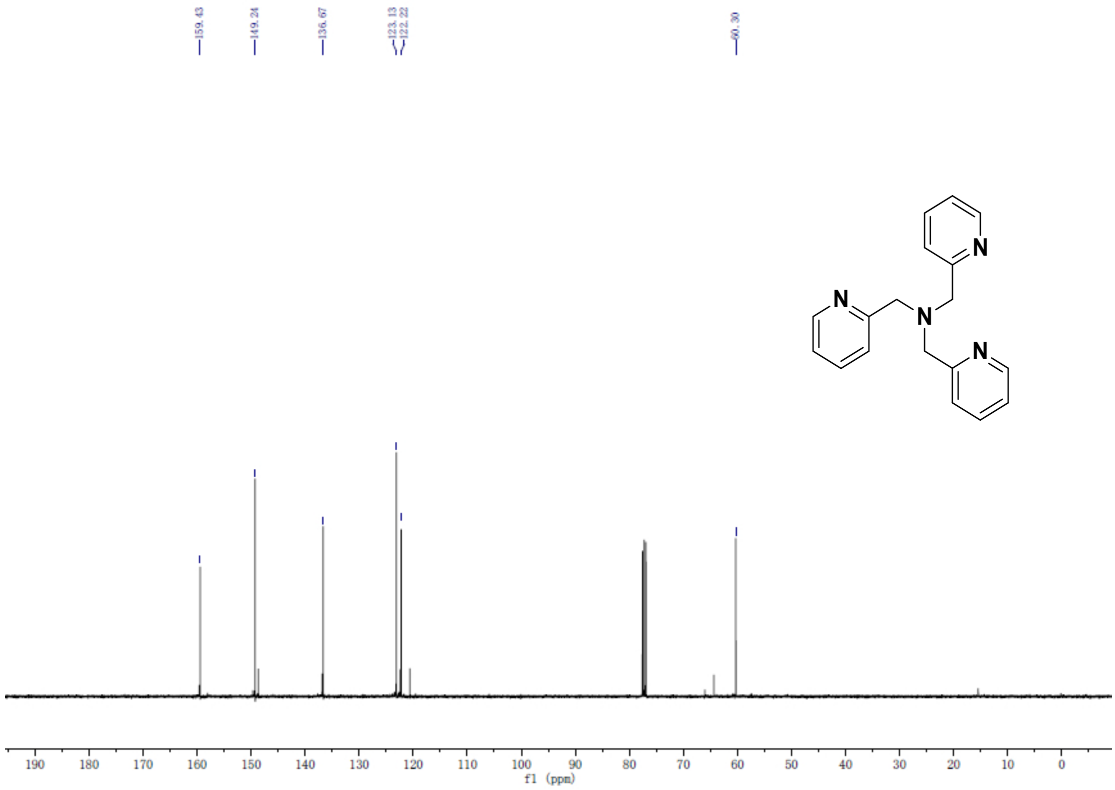

Figure S18. ^{13}C NMR spectrum of Tris(2-pyridylmethyl)amine TPA.

Synthesis of N,N-Bis(2-pyridylmethyl)-N-(2-hydroxybenzyl)amine H(L1):[3]

To a solution of 2-hydroxybenzaldehyde (0.61 g, 5 mmol) in methanol (50 mL) were added bis(2-pyridylmethyl)amine (1.0 g, 5mmol) and a small amount of acetic acid. Sodium cyanotrihydroborate (0.31 g, 5 mmol) in methanol (5 mL) was added dropwise to the resulting solution with stirring. After the solution was stirred for 3 days at 25 °C, it was acidified by adding HCl and then evaporated almost to dryness under reduced pressure. The residue was dissolved in saturated aqueous Na_2CO_3 solution (25 mL) and extracted with $CHCl_3$ (3×50 mL). The combined extracts were dried over anhydrous Na_2SO_4 and filtered. The filtrate on evaporation gave the ligand H(L1) as a colorless oil, which was used for preparation of the complex. Yield: 1.23 g (86%). ^{1}H NMR (400 MHz, $CDCl_3$): δ (ppm): 11.11 (1H), 8.56 (d, J=4.0 Hz, 2H), 7.62 (td, J=7.6; 1.6 Hz 2H), 7.34(d, J=8.0 Hz, 2H), 7.17 (m, 3H), 7.07 (m, 1H), 6.91 (d, J=8.0, 1H), 6.77 (td, J=7.6 Hz 1H), 3.87(s, 4H), 3.79(s, 2H). ^{13}C NMR (400 MHz, $CDCl_3$): 158.37, 157.71, 149.01, 136.87, 130.27, 129.16, 123.33, 122.93, 122.33, 118.98, 116.65, 59.19, 57.06; ESI-MS, $(C19H20N3O)^+$, m/z 306.16; found: 306.1111.

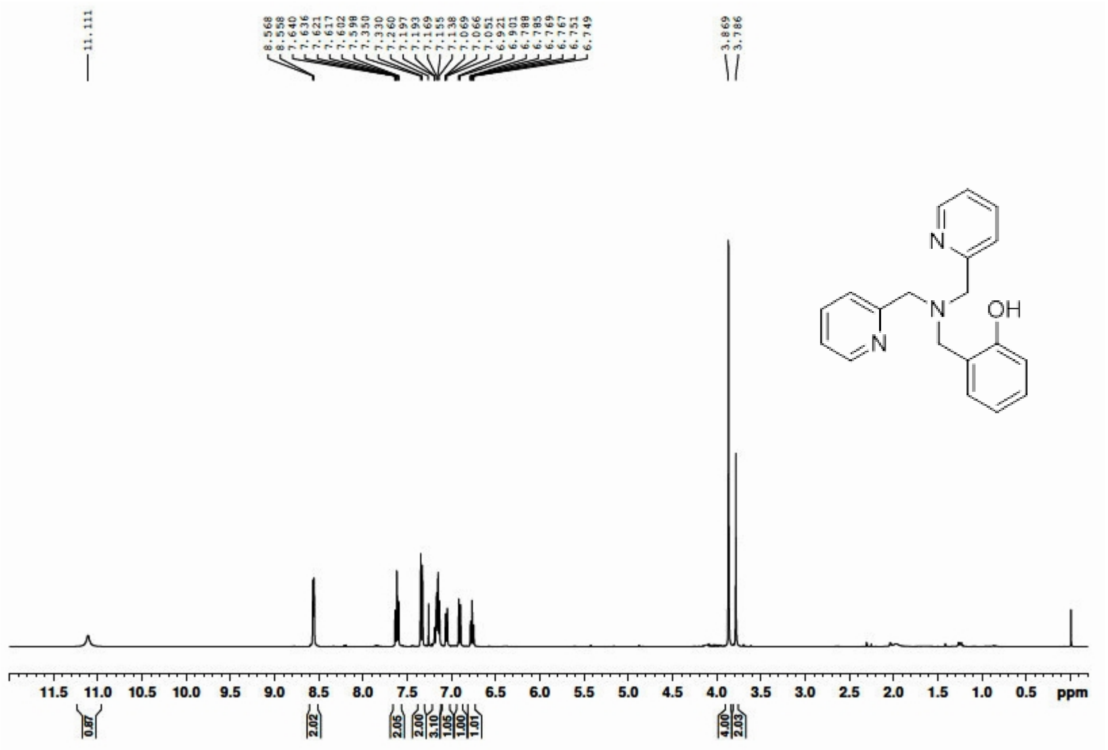

Figure S19. ^{1}H NMR spectrum of N,N-Bis(2-pyridylmethyl)-N-(2-hydroxybenzyl)amine H(L1).

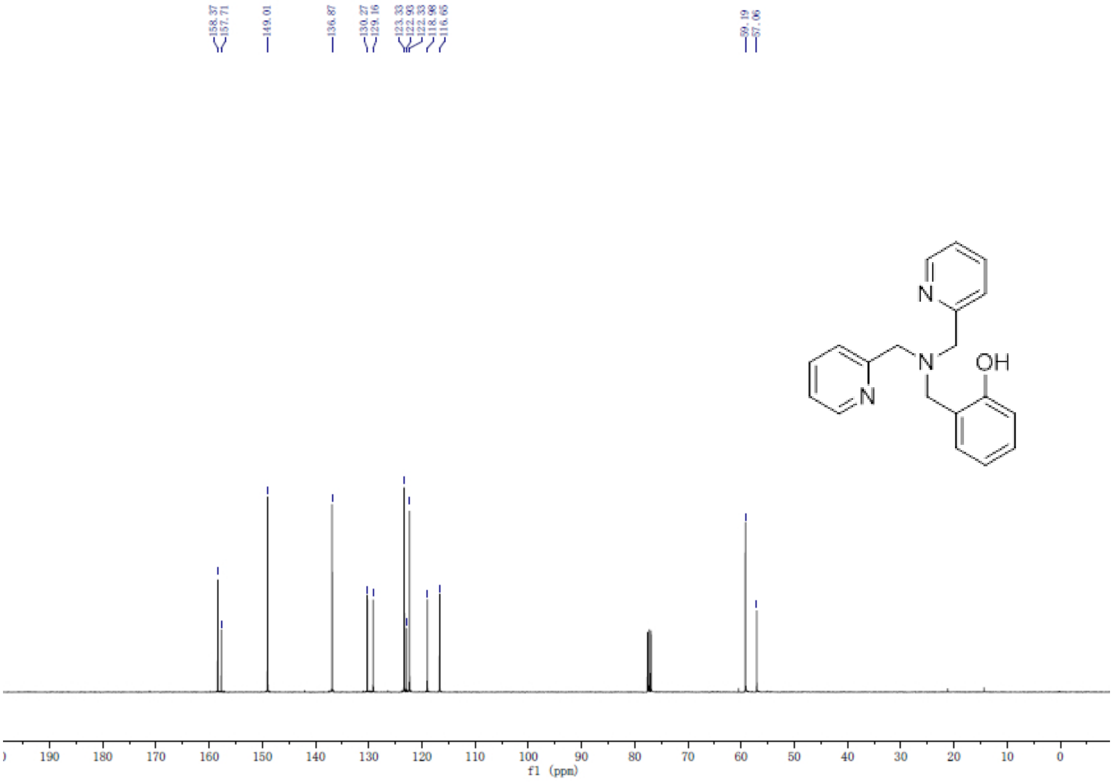

Figure S20. ^{13}C NMR spectrum of N,N-Bis(2-pyridylmethyl)-N-(2-hydroxybenzyl)amine H(L1).

Synthesis of [(TPA)Fe(Cl)$_2$]Cl (1):[4]

A solution of TPA (200 mg, 0.69 mmol) in 2 mL of MeCN was added to a suspension of FeCl$_3$ (112 mg, 0.69 mmol) in 5 mL of MeCN to produce a reddish suspension. After stirring at room temperature for 1 hour, the reaction mixture was filtered to yield a light red solution. Et$_2$O was added to the filtrate to precipitate the compound as a yellow powder (193 mg, 62% yield). The acetonitrile solution of complex **1** exhibits broad EPR signals at g = 2.0145 (S = 1/2) at room temperature. The spectral feature is associated with a octahedral low-spin iron(III) complex. Complex **1** was characterized by ^{1}H NMR in CD$_3$CN, no identifiable signals were obtained, as expected for the paramagnetic ferric iron mode. IR (CM^{-1}): 1606(S), 1485(m), 1443(s), 1289(m), 1159(m), 1097(m), 1054(m), 1025(s), 910(w), 817(w), 765(s), 731(m). Anal. Calcd for C18H18Cl3FeN4: C, 47.77; H, 4.01; N, 12.38; Cl, 23.50; Fe, 12.34%. Found: C, 48.37; H, 4.25; N, 12.70; Cl, 22.59; Fe, 12.06%. ESI-MS. Found: 416.0535. [FeTPACl$_2$]$^+$, $C_{18}H_{18}Cl_2FeN_4^+$, m/z 416.03.

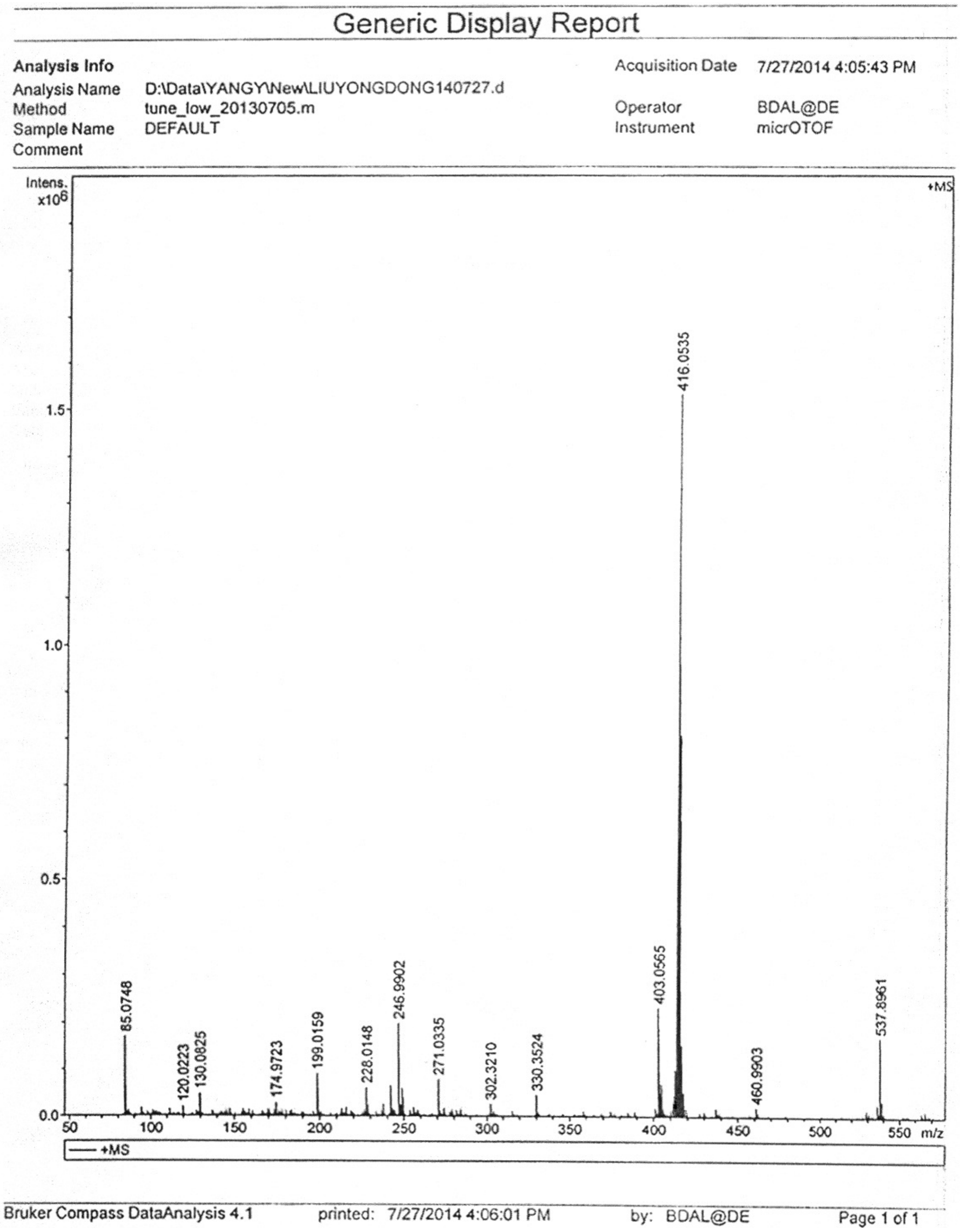

Generic Display Report

Analysis Info		Acquisition Date	7/27/2014 4:05:43 PM
Analysis Name	D:\Data\YANGY\New\LIUYONGDONG140727.d		
Method	tune_low_20130705.m	Operator	BDAL@DE
Sample Name	DEFAULT	Instrument	micrOTOF
Comment			

Bruker Compass DataAnalysis 4.1 printed: 7/27/2014 4:06:01 PM by: BDAL@DE Page 1 of 1

Figure S21. ESI-MS spectrum of complex **1** in CH_3CN.

Synthesis of [(TPA)$_2$Fe$_2$(μ-O)Cl$_2$]Cl$_2$ (2):[5]

A typical preparation of **2** is as follows: TPA (0.145 mg, 0.5 mmol) was dissolved in 20 mL of MeOH and treated with Et_3N (0.31 mL, 2.25 mmol). $FeC1_3$•$6H_2O$ (0.135 g, 0.5 mmol) in a small volume (1-2 mL) of MeOH was added to the resulting solution of TPA. To this resultant red solution was added NaOAc (0.034 g, 0.25

mmol). Single crystals suitable for X-ray crystallography were obtained by vapor diffusion with methanol and diethyl ether. IR (CM^{-1}): 1628 (w), 1604 (s), 1571 (m), 1484 (m), 1313 (w), 1294 (w), 1157 (w), 1100 (m), 1053 (m), 1024 (m), 975 (w), 827(s), 766 (s), 722 (w), 642 (m). The element analysis was tested from the single crystals sample. Anal. Calcd for C36H36Cl4Fe2N8O: C, 48.79; H, 4.55; N, 12.64 Cl, 16.00; Fe, 12.60%. Found: C, 48.67; H, 4.55; N, 12.70; Cl, 16.07; Fe, 12.68%. ESI-MS. Found: 813.1293; $[Fe_2TPA_2(\mu\text{-}O)Cl_3]^+$, $C_{36}H_{36}Cl_3Fe_2N_8O^+$, m/z 813.08.

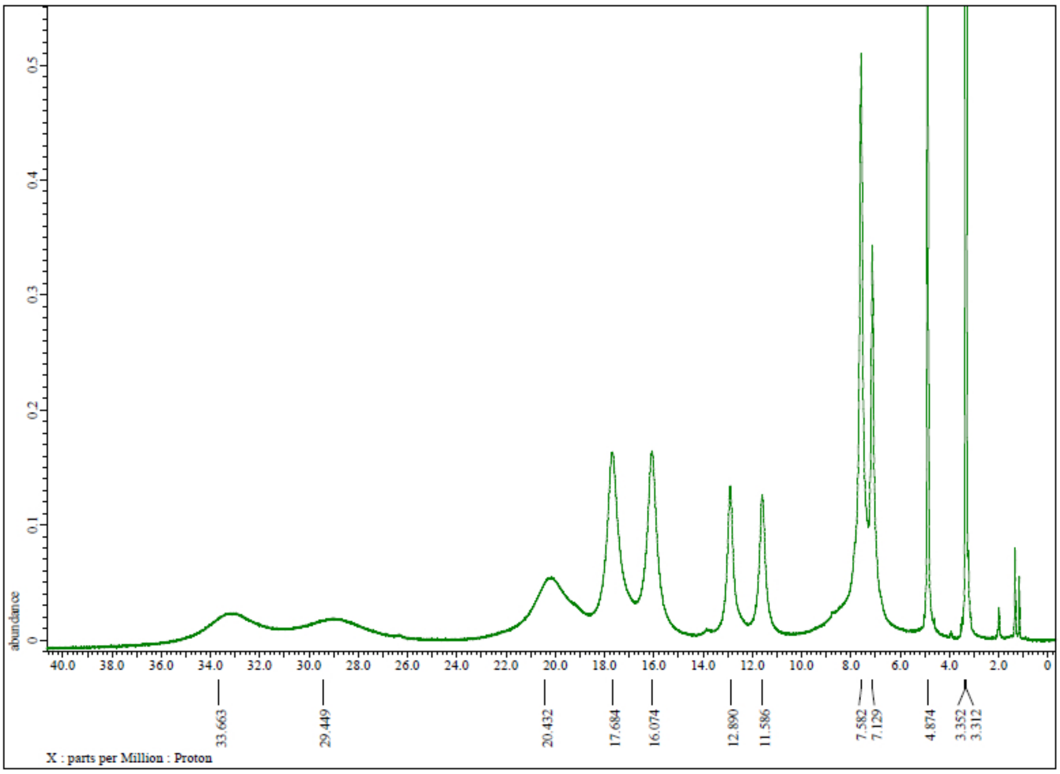

Figure S22. ^{1}H NMR spectrum (300MHz, CD_3OD) of $[(TPA)_2Fe_2(\mu\text{-}O)Cl_2]Cl_2$ (**2**).

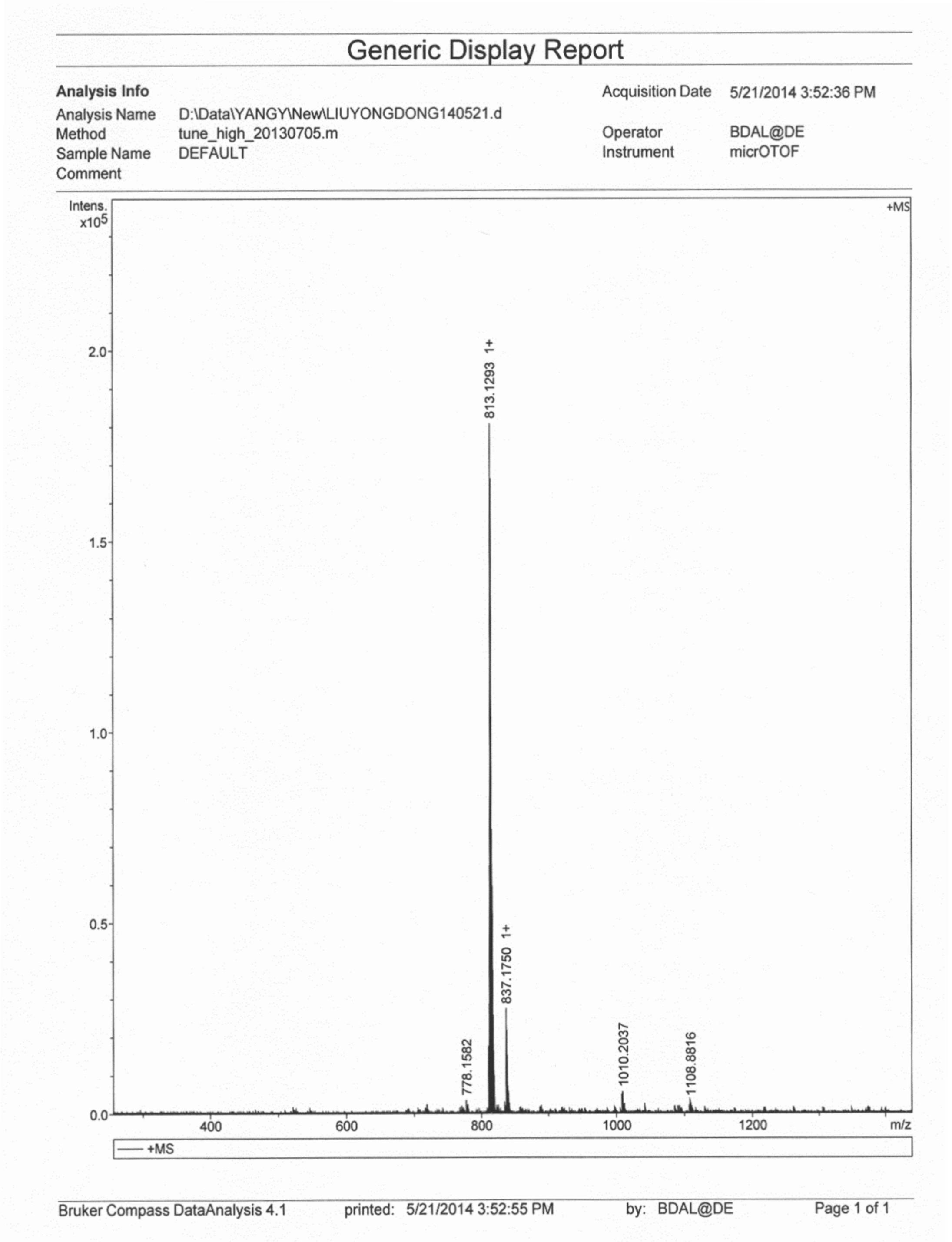

Generic Display Report

Analysis Info

Analysis Name D:\Data\YANGY\New\LIUYONGDONG140521.d
Method tune_high_20130705.m
Sample Name DEFAULT
Comment

Acquisition Date 5/21/2014 3:52:36 PM
Operator BDAL@DE
Instrument micrOTOF

Bruker Compass DataAnalysis 4.1 printed: 5/21/2014 3:52:55 PM by: BDAL@DE Page 1 of 1

Figure S23. ESI-MS spectrum of complex **2** in CH_3OH: 813.1293 $[Fe_2TPA_2(\mu\text{-}O)Cl_3]^+$.

Synthesis of Fe(L1)Cl_2 (3):[3]

The complexes [Fe(L1)Cl_2] were prepared by reaction of a solution of ferric chloride (1.68 g, 6.2 mmol) in methanol (30 mL) to a methanolic solution (60 mL) of an equivalent amount of the ligand H(L1) (6.2 mmol) in the presence of an equivalent amount of triethylamine (Et_3N) (0.63 g, 868μL, 6.2 mmol) in stoichiometric combination. The solution was stirred for an hour to obtain a blue precipitate, which was filtered off, washed with small amounts of cold methanol, and dried in vacuo over P_2O_5. Single crystals suitable for X-ray crystallography were obtained by vapor diffusion with methanol and diethyl ether. The element analysis was tested from the single crystals. IR (CM^{-1}): 1607 (m), 1591 (m), 1572 (w), 1478 (m), 1454 (s), 1441 (m), 1422 (s), 1281 (s), 1097 (w), 1052 (w), 1020 (m), 885 (w), 750 (m), 730 (m). Anal. Calcd for C19H18Cl2FeN3O: C, 52.93; H, 4.21; N, 9.75; Cl, 16.45; Fe, 12.95%; Found: C, 52.77; H, 4.19; N, 9.68; Cl, 16.63; Fe, 12.87%. ESI-MS : m/z 419.2 [Fe(III)L1(CH_3COO)]$^+$.

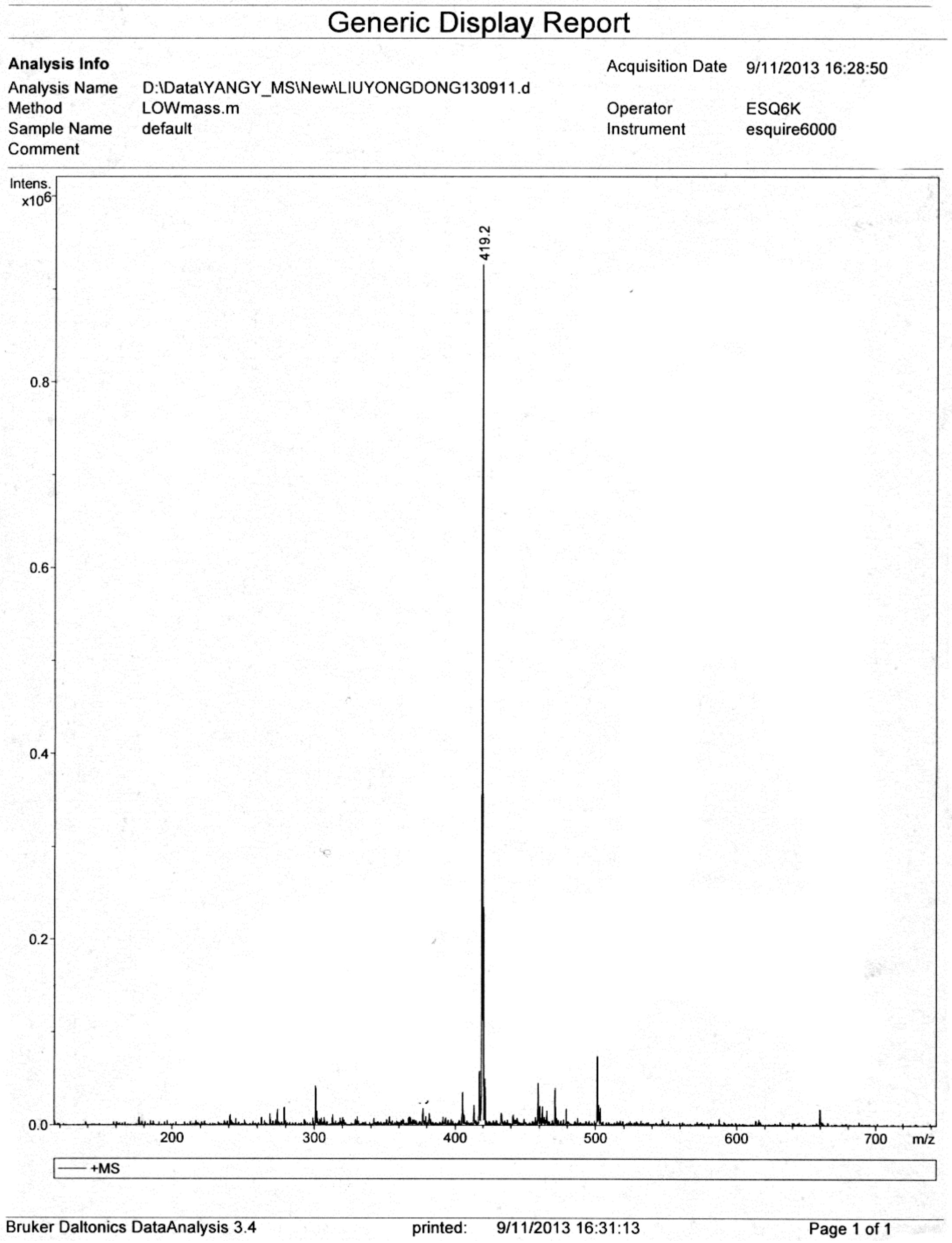

Generic Display Report

Analysis Info

Analysis Name D:\Data\YANGY_MS\New\LIUYONGDONG130911.d
Method LOWmass.m
Sample Name default
Comment

Acquisition Date 9/11/2013 16:28:50
Operator ESQ6K
Instrument esquire6000

Bruker Daltonics DataAnalysis 3.4 printed: 9/11/2013 16:31:13 Page 1 of 1

Figure S24. ESI-MS spectrum of complex **3** in acetate buffer solution: $[FeL1(CH_3COO)]^+$ ($C_{21}H_{21}FeN_3O_3$).

Synthesis of FeTCPP (4):[6]

FeTCPP was prepared by refluxing meso-Tetra(4-carboxyphenyl)porphine(TCPPH) (0.11 mmol) with $FeCl_3 \cdot 6H_2O$ (118 mg, 0.61 mmol) in N,N’-dimethylformamide (17 ml) for 2 hours. DMF was removed by distillation and FeTCPP were precipitated by adding water. The precipitate was dissolved in 0.1 M NaOH solution and reprecipitated by adding 1 M HCl solution. FeTCPP was dissolved in ethanol and recrystallized by solvent evaporation. Finally FeTCPP was dried at room temperature. IR (CM^{-1}): 1701 (s), 1637 (s), 1606 (m), 1488 (m), 1404 (w), 1384 (w), 1320 (w), 1261 (w), 1231 (s), 1108 (w), 1016 (w), 985 (w), 781 (m), 716(m). Anal.Calcd for $C_{48}H_{28}ClFeN_4O_8$: C, 65.51; H, 3.21; N, 6.37; Cl, 4.03; Fe, 6.35%. Found: C, 64.85; H, 3.72; N, 6.12; Cl, 3.89; Fe, 6.16%.

Synthesis of $Fe(bpy)_2Cl_2$ (5):

To a solution of 2,2'-Bipyridine(bpy) (0.310g, 2.0 mmol) in CH_3OH (3 mL) was added $FeCl_3·6H_2O$ (0.270 g, 1.0 mmol) in CH_3OH (2ml). To this red solution was added NaOAc (0.068 g, 0.5 mmol), and the resulting solution was left to stand for a few days at room temperature. The solution was filtered, and then ethyl acetate was added. The brown precipitate obtained was filtered off, dried under vacuum. IR (CM^{-1}): 1629 (w), 1598 (s), 1472 (m), 1314 (s), 1157 (w), 1022 (m), 829 (m), 767 (s), 732 (m), 654 (w). Anal.Calcd for C20H16Cl2FeN4: C, 54.70; H, 3.67; N, 12.76; Cl, 16.15; Fe, 12.72%. Found: C, 54.79; H, 3.81; N, 12.62; Cl, 15.93; Fe, 12.54%.ESI-MS : m/z 184.1 $[Fe(II)(bpy)]^{2+}$ $(C_{20}H_{16}FeN_4)^{2+}$; m/z 403 $[Fe(II)(bpy)Cl]^{+}$ $(C_{20}H_{16}ClFeN_4)^{+}$.

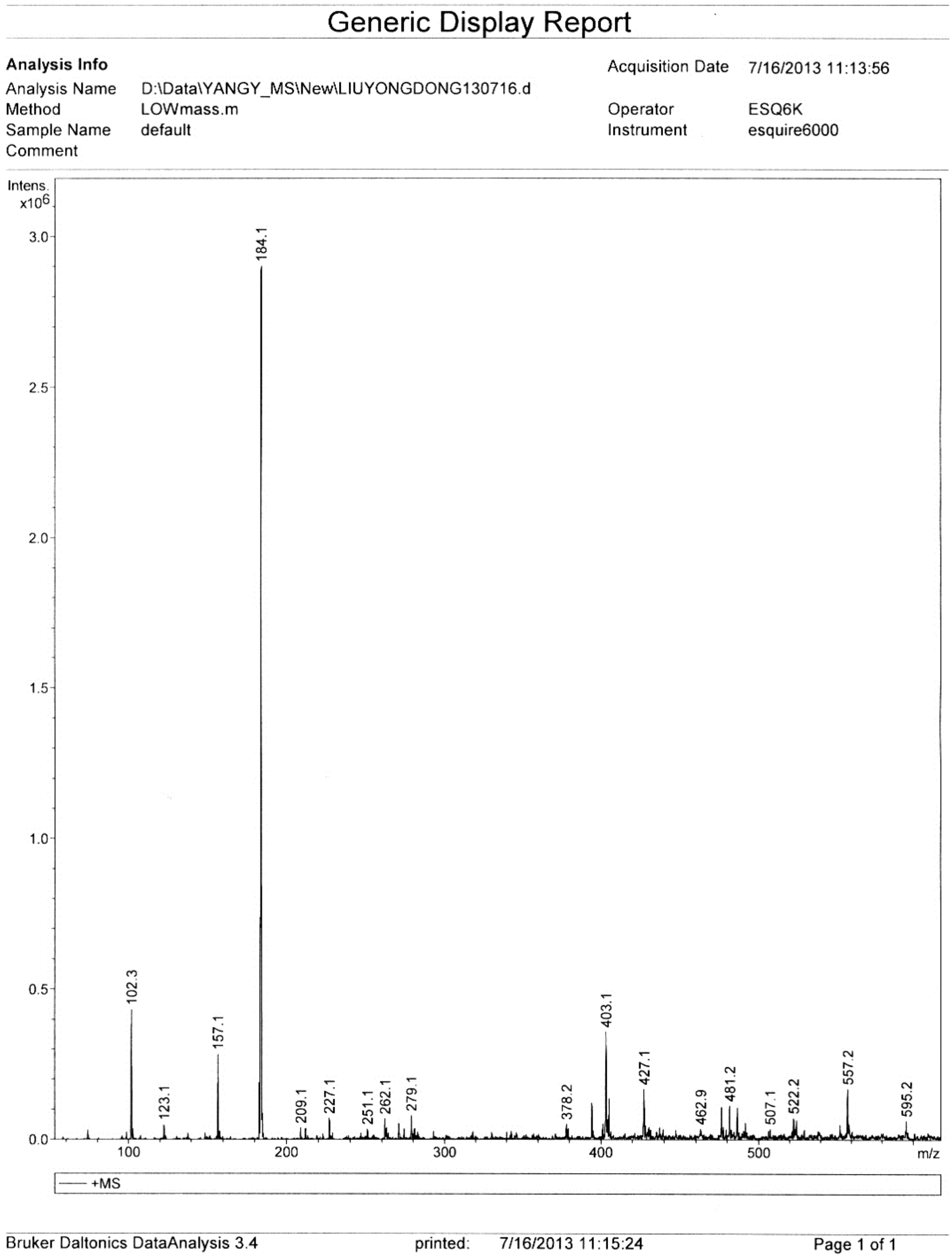

Generic Display Report

Analysis Info

Analysis Name D:\Data\YANGY_MS\New\LIUYONGDONG130716.d
Method LOWmass.m
Sample Name default
Comment
Acquisition Date 7/16/2013 11:13:56
Operator ESQ6K
Instrument esquire6000

Bruker Daltonics DataAnalysis 3.4 printed: 7/16/2013 11:15:24 Page 1 of 1

Figure S25. ESI-MS spectrum of complex **5** in MeOH: [Fe(II)(bpy)]$^{2+}$ ($C_{20}H_{16}FeN_4$); [Fe(II)(bpy)Cl]$^+$ ($C_{20}H_{16}ClFeN_4$)

Synthesis of Fe(phen)$_2$Cl$_2$ (6):

To a solution of 1,10-phenanthroline(phen) (0.396g, 2.0 mmol) in CH_3OH (3 mL) was added $FeCl_3 \cdot 6H_2O$ (0.270 g, 2.0 mmol) in CH_3OH (2ml). A yellow precipitate was produced. The yellow precipitate obtained was filtered off, dried under vacuum.

IR (CM^{-1}): 1618 (w), 1502 (s)，1453 (m), 1411 (m), 1325 (w), 1227 (w), 1053 (m), 890 (m), 842 (s), 811 (s), 723 (m). Anal.Calcd for C24H16Cl2FeN4: C, 59.17; H, 3.31; N, 11.50; Cl, 14.55; Fe, 11.46%. Found: C, 59.30; H, 3.27; N, 11.42; Cl, 14.39; Fe, 11.69%. ESI-MS : m/z 208.1 [Fe(II)(phen)]$^{2+}$; m/z 451 [Fe(II)(phen)Cl]$^{+}$.

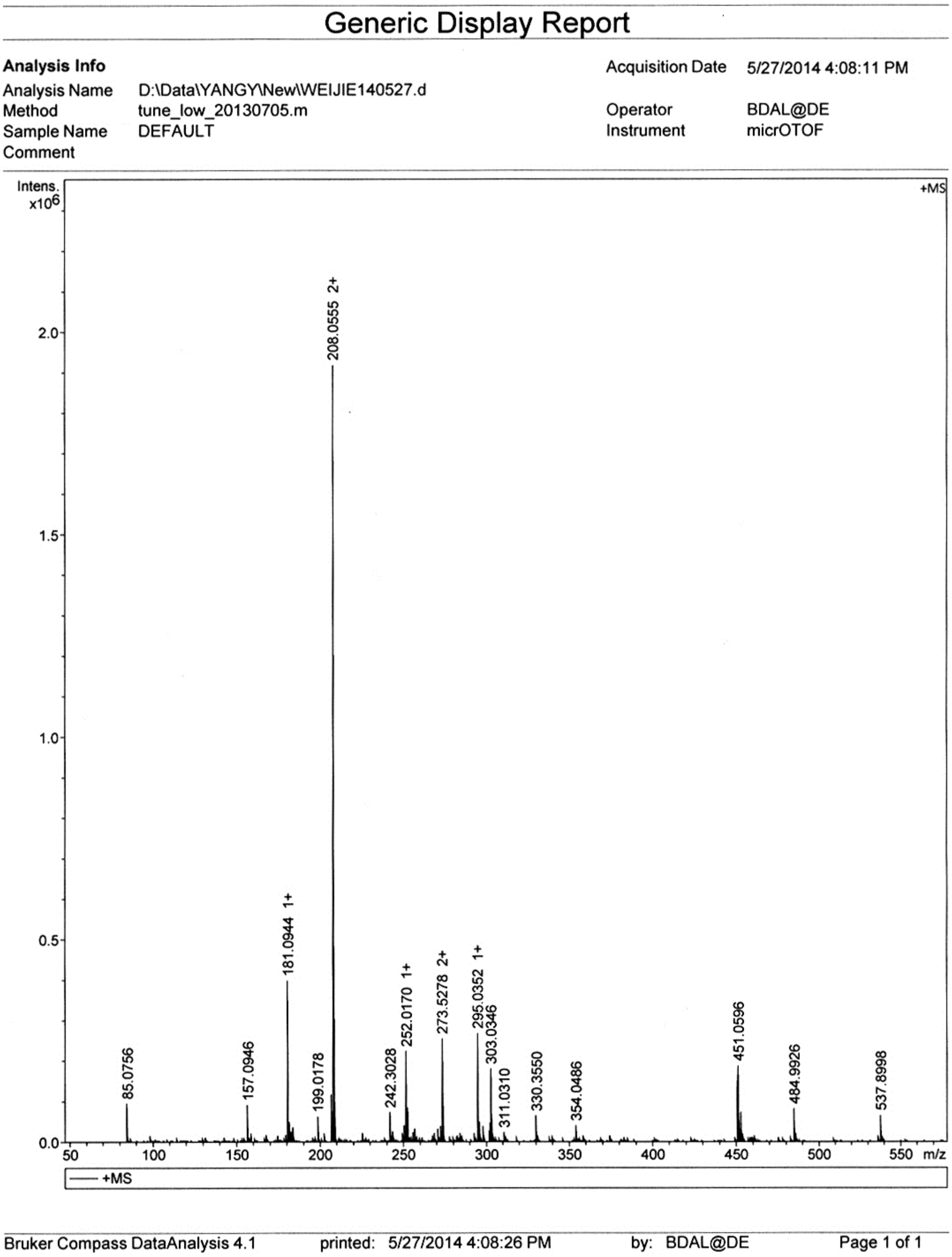

Generic Display Report

Analysis Info		Acquisition Date	5/27/2014 4:08:11 PM
Analysis Name	D:\Data\YANGY\New\WEIJIE140527.d		
Method	tune_low_20130705.m	Operator	BDAL@DE
Sample Name	DEFAULT	Instrument	micrOTOF
Comment			

Bruker Compass DataAnalysis 4.1   printed: 5/27/2014 4:08:26 PM   by: BDAL@DE   Page 1 of 1

Figure S26. ESI-MS spectrum of complex **6** in MeOH: [Fe(II)(phen)]$^{2+}$ ($C_{24}H_{16}FeN_4$); [Fe(II)(phen)Cl]$^{+}$ ($C_{24}H_{16}ClFeN_4$)

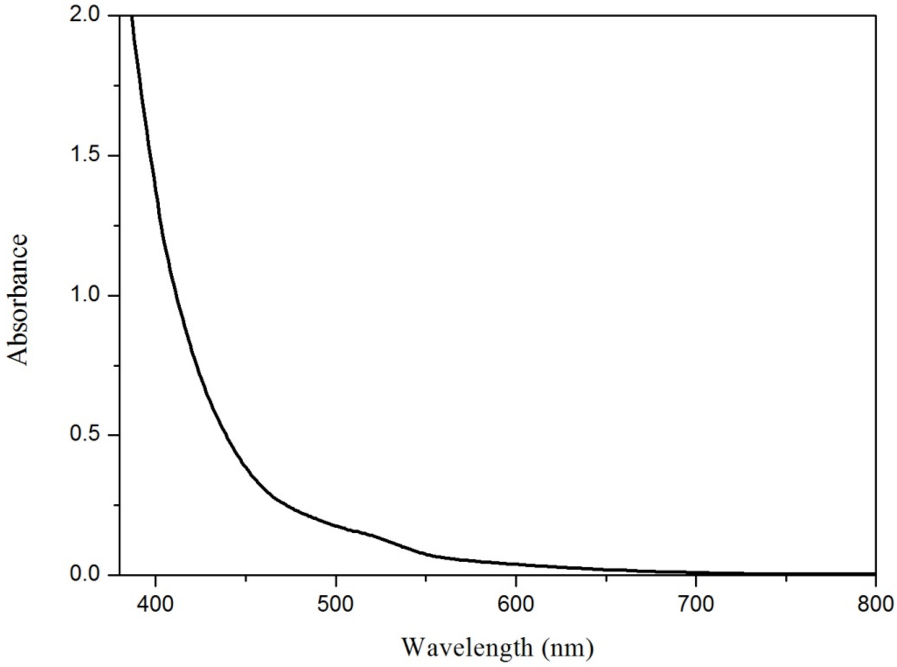

Figure S27. UV-vis spectrum for 1.0 mM of **6** in acetate buffer (0.23 M pH 4.5).

Synthesis of nano-Fe_2O_3:[7]

Fe_2O_3 nanoparticles were prepared according to a published method: ultra-pure water was heated to 100 ^oC. The water was poured into a preheated Pyrex glass beaker. The temperature remained at 100 ^oC. Concentrated (37 wt%) HCl was added to this system to make a 0.002 M HCl solution. The temperature was kept at 90–100 ^oC. Finally $FeCl_3 \cdot 6H_2O$ was dissolved in this hot solution to make a 0.02 M Fe^{3+} solution. The beaker was closed and put into an oven that was preheated to 100 ^oC, where it remained for 1 week. A sample was taken after 24 hours.

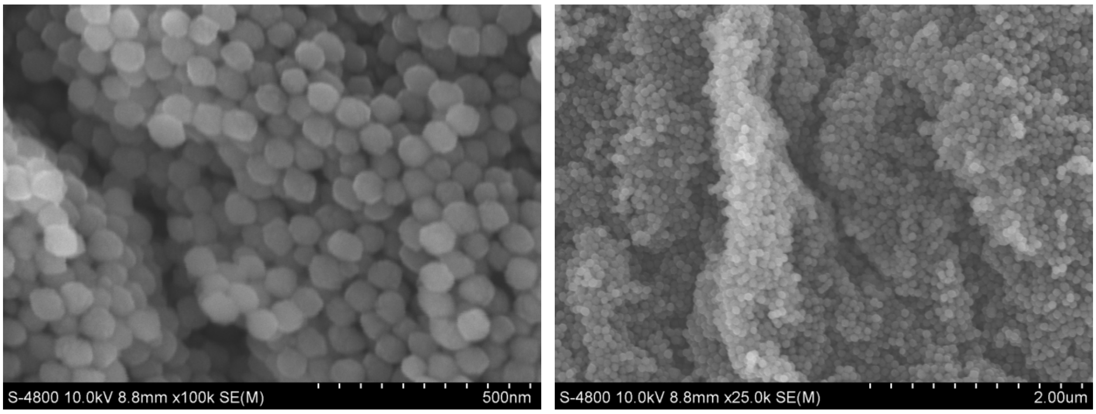

Figure S28. SEM images of nano-Fe_2O_3.

References

1. R. Viswanathan and M. Palaniandavar, *J. Chem. Soc. Dalton. Trans.*, 1995, 1259-1266.
2. D. Schnieders, M. Merkel, S. M. Baldeau and B. Krebs, *Z. Anorg. Allg. Chem.*, 2004, **630**, 1210-1214.
3. R. Mayilmurugan, K. Visvaganesan, E. Suresh and M. Palaniandavar, *Inorg. Chem.*, 2009, **48**, 8771-8783.
4. A. L. Ward, L. Elbaz, J. B. Kerr and J. Arnold, *Inorg. Chem.*, 2012, **51**, 4694-4706.
5. R. E. Norman, S. Yan, L. Que, G. Backes, J. Ling, J. Sanders-Loehr, J. H. Zhang and C. J. O'Connor, *J. Am. Chem. Soc.*, 1990, **112**, 1554-1562.
6. G. G. Oliveros, F. M. Ortega, E. P.Mozo, C. Ferronato. and J.M.Chovelon, *Open. Mater. Sci. J*, 2010, **4**, 15.
7. T. P. Raming, A. J. A. Winnubst, C. M. van Kats and A. P. Philipse, *J. Colloid Interface Sci.*, 2002, **249**, 346-350.